Available online at www.sciencedirect.com

SciVerse ScienceDirect

Ceramics International 38 (2012) 6021–6026

CERAMICS INTERNATIONAL

www.elsevier.com/locate/ceramint

Short communication

Effect of pre-oxidation on the microstructure, mechanical and dielectric properties of highly porous silicon nitride ceramics

Rubing Zhang *, Daining Fang, Xiangmeng Chen, Yongmao Pei

State Key Lab. for Turbulence and Complex Systems (LTCS), College of Engineering, Peking University, Beijing 100871, PR China

Received 1 March 2012; received in revised form 22 March 2012; accepted 23 March 2012
Available online 1 April 2012

Abstract

Highly porous Si_3N_4 ceramics have been fabricated via freeze casting and sintering. The as-sintered samples were pre-oxidized at 1200–1400 °C for 15 min. The effect of pre-oxidation temperature on the microstructure, flexural strength, and dielectric properties of porous Si_3N_4 ceramics were investigated. As the pre-oxidation temperature increased from 1200 °C to 1400 °C, firstly, the flexural strength of the pre-oxidized specimens remained almost constant at 1200 °C, and then decreased to 14.2 MPa at 1300 °C, but finally increased to 25.6 MPa at 1400 °C, while the dielectric constant decreased gradually over the frequencies ranging from 8.2 GHz to 12.4 GHz. This simple process allows porous Si_3N_4 ceramics to have ultra-low dielectric constant and moderate strength, which will be feasible in broadband radome applications at high temperatures.

Keywords: B. Porosity; C. Dielectric properties; C. Mechanical properties; D. Si_3N_4

1. Introduction

Porous ceramic materials with a tailored microstructure have potential applications as structural components because of their unique properties, such as light weight, good strain and damage tolerance, and good thermal shock resistance. Silicon nitride ceramics are among the well-developed materials through such approaches. Porous Si_3N_4 ceramics with a microstructure of β-Si_3N_4, a high-temperature phase with interconnected fibrous β-Si_3N_4 grains bonded together and reinforcing each other, are of practical importance. These ceramics are suitable for various promising applications at high temperatures because of their excellent mechanical properties at room and elevated temperatures, good thermal shock resistance, and excellent dielectric properties [1–5].

Porous Si_3N_4 ceramics can be prepared in different ways, such as adding fugitive substance [6], freeze casting [7], carbothermal nitridation [5], combustion synthesis [8], in situ reaction bonding [9], and gel casting [10], among others. For example, porous Si_3N_4 ceramics with porosities of 19.4–42.6% were fabricated through the oxidation bonding process, which attained a high flexural strength of 43–137 MPa, a low dielectric constant of 3.1–4.6, and a low dielectric loss of $(2.9–4.3) \times 10^{-3}$ at 1 GHz [11]. Porous $Si_3N_4/(Si_3N_4 + BN)$ sandwich ceramics fabricated via tape casting and hot pressing attained a moderate flexural strength of 53.4 MPa and a low dielectric constant of 3.48 at 1 GHz [12]. However, high porosity decreases the resistance of porous Si_3N_4 ceramics to moisture and mechanical erosion. Therefore, the fabrication of porous Si_3N_4 ceramics with a dense surface is necessary.

Many researchers have attempted to create a dense surface on porous Si_3N_4 ceramics. Recently, a porous Si_3N_4 ceramic has been fabricated via oxidation of Si_3N_4 preform, which attained a high-flexural strength of 137 MPa with a dielectric constant of 4.6 and dielectric loss of 2.9×10^{-3} at 1 GHz [9]. Liu et al. fabricated a dense/porous Si_3N_4 composite using the chemical vapor infiltration process. The composite attained an acceptable strength of 113 MPa and a low-dielectric constant of approximately 4.2–4.3 [13]. Yin and co-workers [14] fabricated a dense/porous Si_3N_4–SiO_2 composite ceramic via a novel process combining oxidation bonding with sol–gel infiltration-sintering. As the content of sol–gel infiltration increased, the dielectric constant of the dense/porous Si_3N_4–SiO_2 composite ceramic increased from 3.08 to 3.80, whereas the dielectric loss

---

* Corresponding author. Tel.: +86 01062757417; fax: +86 01062757417.
E-mail address: rbzhang@pku.edu.cn (R. Zhang).

0272-8842/$36.00 © 2012 Elsevier Ltd and Techna Group S.r.l. All rights reserved.
http://dx.doi.org/10.1016/j.ceramint.2012.03.056

decreased. Li et al. [15] fabricated a porous Si_3N_4–SiC(BN) ceramic via precursor infiltration pyrolysis. As the annealing temperature increased from 900 °C to 1800 °C, the mechanical properties of porous Si_3N_4–SiC(BN) ceramics exhibited slight improvement, whereas the average real part of porous Si_3N_4–SiC(BN) ceramics increased from 6.91 to 26.20. Several attempts have been proposed to improve the mechanical properties by introducing a dense surface. However, these attempts also resulted in higher dielectric constants of porous Si_3N_4 ceramics. Porous Si_3N_4 ceramics need to maintain ultra-low dielectric constants for broadband radome applications at high temperatures.

Many recent studies have induced a self-crack-healing ability to increase the reliability of structural ceramics by pre-oxidation. Moreover, several works reported on the crack-healing behavior of engineering ceramics, such as Al_2O_3/SiC composites [16,17], Si_3N_4 matrix composites [18,19], ZrB_2–SiC ceramics [20,21], and ternary carbide Ti_3AlC_2 ceramics [22]. Pre-oxidation has been demonstrated to increase mechanical properties, hot corrosion resistance, and thermal shock behavior by forming a dense surface, which could blunt or heal surface flaws. The pre-oxidation and crack-healing behavior of hot-pressed ZrB_2–20 vol.% SiCw composites as a function of temperature and time were studied by Zhang et al. [21]. The flexural strength improved after pre-oxidation, with a maximum increase of strength (15%) for samples after pre-oxidizing at 800 °C for 180 min. Liu et al. [23] studied the effect of pre-oxidation on the hot corrosion behavior of non-oxide Ti_3SiC_2 ceramics in a mixture of 75 wt.% Na_2SO_4 + 25 wt.% NaCl melts at 850 °C. The results indicated that the hot corrosion resistance of the material could be improved greatly by pre-oxidation treatment. Zhang and co-workers [24] studied the effect of pre-oxidation on the thermal shock behavior of $Zr_2Al_4C_5$–20 vol.% SiC composites via a water-quenching technique. The pre-oxidized $Zr_2Al_4C_5$–20 vol.% SiC composites exhibited great improvement in thermal shock resistance compared with the as-sintered specimens.

However, whether pre-oxidation could also improve the mechanical and dielectric properties of porous ceramics is yet to be determined. To the best of our knowledge, few studies in the open literature have been conducted to determine the effect of pre-oxidation on the mechanical and dielectric properties of porous ceramics. In this work, dense/porous Si_3N_4 composite ceramics with high mechanical properties and low dielectric constant were attained by employing the pre-oxidation process. The effect of process parameters on the composition, microstructure, and mechanical and dielectric properties of the porous Si_3N_4 ceramics were measured and analyzed.

2. Experimental procedures

Slurries were prepared by mixing distilled water with 0.3 wt% ammonium polymethacrylate anionic dispersant (Sigma–Aldrich Trading Co., Ltd., Shanghai, China), glycerol (10 wt.% of solvent), 5 wt.% Y_2O_3 (Sinopharm Chemical Reagent Co., Ltd., Shanghai, China), 3 wt.% Al_2O_3 (Sinopharm Chemical Reagent Co., Ltd., Shanghai, China) and Si_3N_4 (Junyu Ceramic Co., Ltd., Shanghai, China). Slurries were ball-milled with alumina balls for 12 h and de-aired by stirring in a vacuum desiccator. The Si_3N_4 powder consisted of 95 wt% α-Si_3N_4 and 5 wt% β-Si_3N_4, and had a mean diameter of 1.5–2.0 μm. The solid loading of the slurries were fixed to 25 vol.%. Highly porous Si_3N_4 ceramics have been fabricated by freeze casting and sintering. The detailed freeze casting process can be found in our previous work [7]. The green compacts were carefully placed into a graphite crucible with a silicon nitride-based powder bed and sintered in a graphite resistance furnace at 1800 °C for 60 min under a 0.05 MPa nitrogen atmosphere. Both the heating and cooling rates were 5 °C/min.

The pre-oxidation process was carried out in a conventional furnace under air atmosphere. In order to eliminate the effect of thermal shock on mechanical properties, the specimens were heated at ~10 °C/min to the target temperature, held at the target temperature for 15 min, and then left cooling freely inside the furnace.

Porous Si_3N_4 samples of 3 mm × 4 mm × 35 mm were cut off from the as-sintered and pre-oxidized ceramics, and were loaded with a testing machine (Instron 5569, Instron corp., Canton, USA) to test the flexural strength, with a crosshead speed of 0.05 mm/min. All flexural bars were machined with the tensile surface perpendicular to the freezing direction. In order to obtain the average value, more than six samples of each measurement were chosen. The as-prepared and pre-oxidized products were coated with a thin layer of gold and characterized in a scanning electron microscope (FEI Quanta 200, FEI Company, Hillsboro, USA). The dielectric property test is based on measurements of the reflection and transmission moduli between 8.2 and 12.4 GHz, in the fundamental waveguide mode, using standard samples (22.86 mm × 10.16 mm × 3 mm for 8.2–12.4 GHz, Agilent E8326B PNA series network analyzer, USA).

3. Results and discussion

3.1. Microstructure of porous Si_3N_4

Fig. 1(a) shows the typical microstructure of the porous Si_3N_4 ceramics with 25 vol.% solid content obtained through freeze-casting and sintering. The actual porosity of the porous Si_3N_4 ceramics is approximately 62%. As shown in Fig. 1(a), numerous fibrous grains protruding from the internal walls of the macroscopic aligned channels were present in the porous Si_3N_4 samples. The estimated aspect ratio of the fibrous grains is approximately 8, and the average grain size is approximately 4 μm in length and 0.5 μm in width. As shown in Fig. 1(a), the rod-like β-Si_3N_4 particles in the porous Si_3N_4 ceramics intercross with each other to form many open pores that connect well with each other. After pre-oxidation at 1200 °C for 15 min, both α-Si_3N_4 and β-Si_3N_4 were bonded by amorphous SiO_2 from the oxidation of Si_3N_4, which coated the β-Si_3N_4 particles and was well-distributed in the porous Si_3N_4 ceramics [Fig. 1(b)]. This result is supported by the fact that only amorphous SiO_2 can be found in porous Si_3N_4 ceramics by

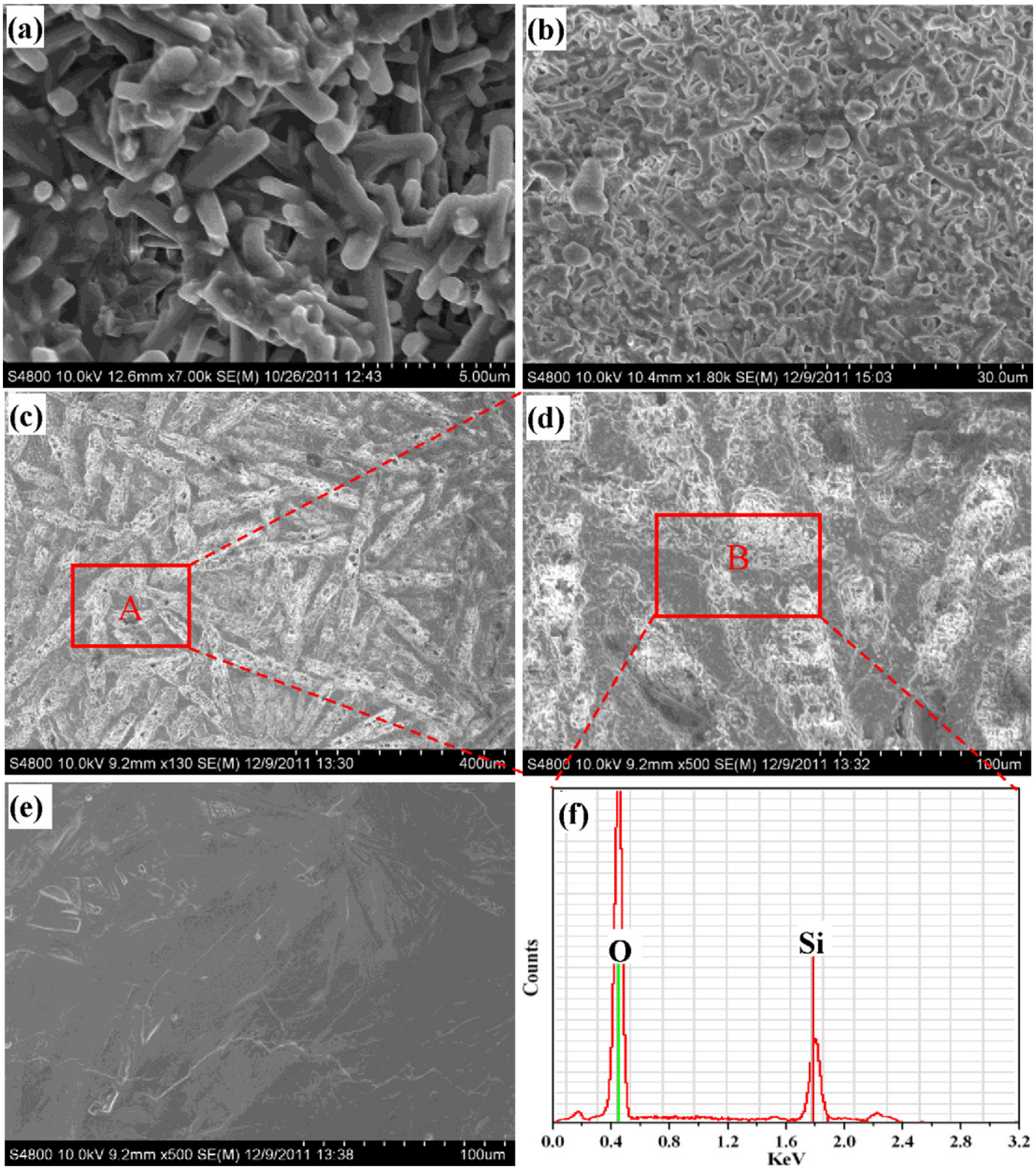

Fig. 1. Typical SEM micrographs of porous Si_3N_4 ceramics after pre-oxidation at different temperatures: (a) as-sintered; (b) 1200 °C; (c) 1300 °C; (d) high-magnification of zone A; (e) 1400 °C and (f) EDS of zone B.

oxidation-bonding processes below 1250 °C. Furthermore, cristobalite peaks would appear when the temperature reaches 1300 °C [14,25].

Fig. 1(c) presents the surface morphology of porous Si_3N_4 ceramics after pre-oxidation at 1300 °C for 15 min. Rod-like β-Si_3N_4 particles were not observed because of the formation of a relatively continuous oxide layer (Fig. 1(c)). Energy dispersive spectrometry (EDS) analysis showed that the surface layer was primarily composed of Si and O (Fig. 1(f)). Based on the above results, we can conclude that Si_3N_4 begins to oxidize to cristobalite at 1300 °C and that the oxidation products should be amorphous SiO_2 and cristobalite. Moreover, rod-like nubbles were found surrounding SiO_2 (Fig. 1(c)). A high-magnification scanning electron micrograph of the rod-like nubbles is shown in Fig. 1(d). The internal walls of the nubbles exhibited small pores. The nubbles were healed incompletely by the viscous liquid phase. This phenomenon can be explained through the convection mechanism in liquid oxide films proposed by Karlsdottir et al. [26]. As the temperature approaches 1300 °C, SiO_2 is much more viscous. Thus, a silica-rich liquid surface layer with no remaining Si_3N_4 should be present at the surface. However, the dendritic pore structure was parallel to the freezing direction in the as-sintered porous Si_3N_4 ceramics, which was too big to be healed completely by the viscous liquid phase during pre-oxidation at 1300 °C.

As the pre-oxidation temperature increased to 1400 °C, the surface morphology changed greatly compared with the 1300 °C/15 min samples (Fig. 1(e)). Rod-like β-Si_3N_4 particles and dendritic pore structure were not observed; the surface was healed completely by the formation of a continuous dense oxide layer. The surface of the sample was dense and smooth. EDS analysis revealed that this dense layer was primarily composed of Si and O (not shown here, results similar with Fig. 1(f)). The results obtained in this work suggest that a dense layer formed by the viscous glass oxidation product can heal the porosity of exposed surfaces during the pre-oxidation process.

3.2. Mechanical properties of porous Si_3N_4 ceramics

The flexural strength of the pre-oxidized porous Si_3N_4 ceramics are affected by many parameters, including material composition, porosity, pore shape, pore size, wall thickness, and wall density, which are mainly determined by fabrication processes. However, considering all the parameters is difficult because they are interdependent. Moreover, all the parameters affect flexural strength via the microstructure, especially during sintering and pre-oxidation processes. In this study, highly porous Si_3N_4 ceramics have been fabricated and pre-oxidized at 1200–1400 °C for 15 min. The relationship between pre-oxidation temperature and flexural strength was plotted (Fig. 2). As shown in Fig. 2, the flexural strength of the obtained porous Si_3N_4 ceramics is greatly affected by the pre-oxidation temperature. The flexural strength of the as-sintered and polished specimens was approximately 33.5 MPa (Fig. 2). As the pre-oxidation temperature increased from 1200 °C to 1400 °C, the average flexural strength of the pre-oxidized specimens first increased from 33.5 MPa to 34.2 MPa, decreased from 34.2 MPa to 14.2 MPa, and then finally increased from 14.2 MPa to 25.6 MPa. The optimum pre-oxidation temperature was 1200 °C. The flexural strength of the 1200 °C/15 min samples was higher than that of the as-sintered and polished specimens (33.5 MPa). In addition, relatively low gas pressure (0.05 MPa) was used in this study to sinter the porous Si_3N_4 ceramics in a graphite resistance furnace. Therefore, the content of elongated β-Si_3N_4 grains is relatively low, which may be the main reason for the moderate flexural strength of the as-sintered porous Si_3N_4 ceramics. Its mechanical properties could be further improved by increasing the gas pressure of N_2, and further work is in progress.

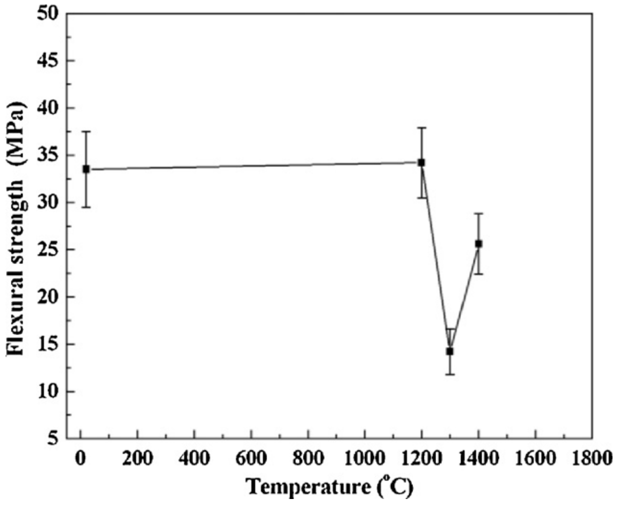

Fig. 2. Effect of pre-oxidation temperature on the flexural strength of porous Si_3N_4 ceramics.

Both the retained elongated β-Si_3N_4 grains and the densification dominate the flexural strength. As shown in Fig. 1(b), both α-Si_3N_4 and β-Si_3N_4 were bonded by amorphous SiO_2 from the oxidation of Si_3N_4 at 1200 °C. In addition, the β-Si_3N_4 grains decreased in size, and the particles were in contact with each other via the oxidation-derived silica. The porous Si_3N_4 ceramics were fractured intergranularly because of the increased bonding between grains. Therefore, the specimens pre-oxidized at 1200 °C for 15 min exhibited improved flexural strength compared with the as-sintered samples because of the content of elongated β-Si_3N_4 grains, thicker necks, and lower porosity.

When the pre-oxidation temperature increased to 1300 °C, the flexural strength decreased to 14.2 MPa. Numerous small pores were formed by the release of gaseous N_2 and SiO during the acute oxidation of Si_3N_4 particles (Fig. 1(c)). Moreover, the retained elongated β-Si_3N_4 grains decreased, and the Si_3N_4 particles were engulfed by the thicker silica necks, which resulted in a significant decrease in flexural strength compared with the as-sintered sample.

As the pre-oxidation temperature increased to 1400 °C, the flexural strength correspondingly increased from 14.2 MPa at 1300 °C to 25.6 MPa. As shown in Fig. 1(e), the surface of the samples was healed completely by the silica phase because of the formation of a continuous dense oxide layer. The flexural strength of the samples was lower than that of the as-sintered and 1200 °C/15 min samples but higher than that of the 1300 °C/15 min samples. The presence of the least-elongated β-Si_3N_4 grains was the main reason for the decrease in flexural strength compared with that of the as-sintered and 1200 °C/15 min samples. However, the strengthening effect of the increase in porosity is more prominent compared with that of the 1300 °C/15 min samples. Therefore, the flexural strength was mainly affected by the competitive effect of Si_3N_4 oxidation degree, bonding necks between particles, porosity, and micro-cracks (mostly caused by cristobalite).

3.3. Dielectric properties of porous Si_3N_4 ceramics

The dielectric constant of porous Si_3N_4 with different pre-oxidation temperatures at 1200–1400 °C for 15 min was measured in the frequency range of 8.2–12.4 GHz. The corresponding profiles are presented in Fig. 3. As shown in Fig. 3, all the materials exhibited reasonably stable and ultra-low dielectric constant. The dielectric constant of the as-sintered porous Si_3N_4 samples was 2.63. However, porous Si_3N_4 ceramics with different pre-oxidation temperatures at 1200–1400 °C for 15 min had lower dielectric constants, and their corresponding dielectric constants at 10 GHz were 2.38, 2.22, and 1.93, respectively.

The overall dielectric constant of porous Si_3N_4 ceramics is highly affected by oxidation-derived silica (amorphous or crystalline), residual Si_3N_4, and pores. According to the mixture rule [27], the dielectric constant of the two-phase composite is calculated as:

$$\varepsilon_0^k = \nu_1\varepsilon_1^k + \nu_2\varepsilon_2^k \quad (1)$$

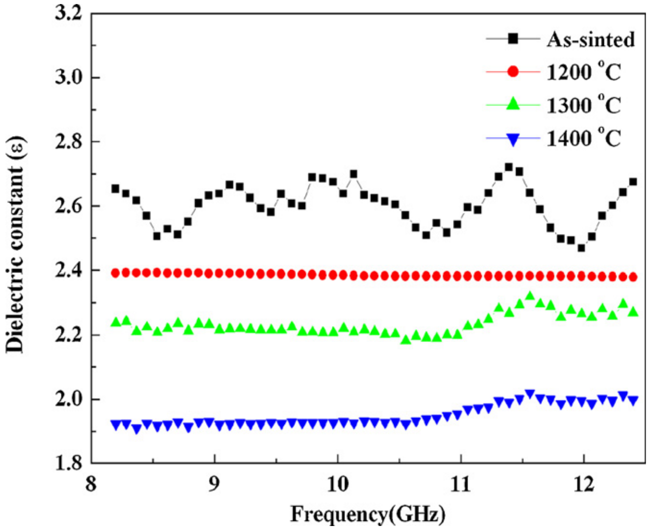

Fig. 3. Effect of pre-oxidation temperature on the dielectric constant of porous Si_3N_4 ceramics in the frequency range of 8.2–12.4 GHz.

where ε_0, ε_1 and ε_2 are the dielectric constant of the composite, phase 1 and phase 2, respectively; ν_1 and ν_2 are the volume fraction of each phase; k is the constant. In addition, the dielectric constant of the porous material can be related to that of the fully dense material simply as:

$$\varepsilon_p = \varepsilon^{(1-p)} \tag{2}$$

where ε_p and ε are the dielectric constant of the porous and fully dense materials, respectively; p is the porosity [28]. In this study, the dielectric constant was mainly affected by the oxidation-derived silica (amorphous or crystalline) and residual Si_3N_4. The high oxidation degree of Si_3N_4 can reduce the dielectric constant greatly because the dielectric constant of silica is lower than Si_3N_4. Although the porosity decreased evidently as the pre-oxidation temperature increased from 1200 °C to 1400 °C, the dielectric constant of the samples at 10 Hz decreased from 2.63 to 1.93.

Compared with some traditional techniques, the present approach in improving the mechanical and dielectric properties of highly porous Si_3N_4 ceramics via pre-oxidation has some advantages. First, the pre-oxidation process is simple. Second, this attempt not only improves the mechanical properties by introducing a dense surface but also lowers the dielectric constant of porous Si_3N_4 ceramics. Finally, the forming dense surface could improve the resistance of porous Si_3N_4 ceramics to moisture and mechanical erosion. Consequently, the pre-oxidation process provides a novel method for the fabrication of porous Si_3N_4 ceramics with high strength and ultra-low dielectric constants.

4. Conclusions

In this paper, the pre-oxidation process was proposed to improve the mechanical and dielectric properties of highly porous Si_3N_4 ceramics. The microstructure, flexural strength, and dielectric properties of porous Si_3N_4 ceramics as functions of pre-oxidation temperature were studied. As the pre-oxidation temperature increased from 1200 °C to 1400 °C, firstly, the average flexural strength of the pre-oxidized specimens remained almost constant at 1200 °C, and then decreased to 14.2 MPa at 1300 °C, but finally increased to 25.6 MPa at 1400 °C, while the dielectric constant at 10 GHz decreased from 2.38 to 1.93. The mechanical and dielectric properties were primarily affected by the competitive effect of the Si_3N_4 oxidation degree, bonding necks between particles, porosity, and microcracks (mostly caused by cristobalite). The ultra-low dielectric constant and moderate strength of the porous Si_3N_4 ceramics fabricated via pre-oxidation have excellent potential for applications in broadband radomes at high temperatures.

Acknowledgments

This work was supported by the National Natural Science Foundation of China (91016021 and 11102003) and China Postdoctoral Science Foundation Funded Project (20110490196). Support by the National Basic Research Program of China (G2010CB832701) was also acknowledged.

References

[1] F.L. Riley, Silicon nitride and related materials, Journal of the American Ceramic Society 83 (2) (2000) 245–265.
[2] Y. Inagaki, N. Kondo, T. Ohji, High performance porous silicon nitrides, Journal of the European Ceramic Society 22 (2002) 2489–2494.
[3] D. Aranzazu, H. Stuart, Characterization of porous silicon nitride materials produced with starch, Journal of the European Ceramic Society 24 (2) (2004) 413–419.
[4] T. Fukasawa, Z.Y. Deng, M. Ando, Synthesis of porous silicon nitride with unidirectionally aligned channels using freeze-drying process, Journal of the American Ceramic Society 85 (9) (2002) 2151–2155.
[5] S.Y. Shan, J.F. Yang, J.Q. Gao, W.H. Zhang, Z.H. Jin, Porous silicon nitride ceramics prepared by reduction–nitridation of silica, Journal of the American Ceramic Society 88 (9) (2005) 2594–2596.
[6] F.S. Li, W.C. Zhou, H.J. Hu, F. Luo, D.M. Zhu, High performance porous Si_3N_4 ceramics prepared by coated pore-forming agent method, Ceramics International 35 (2009) 3169–3173.
[7] R.B. Zhang, D.N. Fang, Y.M. Pei, L.C. Zhou, Microstructure, mechanical and dielectric properties of highly porous silicon nitride ceramics produced by a new water-based freeze casting, Ceramics International (2012), http://dx.doi.org/10.1016/j.ceramint.2012.01.012.
[8] D.Y. Chen, B.L. Zhang, H.R. Zhuang, W.L. Li, Combustion synthesis of network silicon nitride porous ceramics, Ceramics International 29 (4) (2003) 363–364.
[9] Y.F. Xia, Y.P. Zeng, D.L. Jiang, Dielectric and mechanical properties of porous Si_3N_4 ceramics prepared via low temperature sintering, Ceramics International 35 (2009) 1699–1703.
[10] J.L. Yu, H.J. Wang, J. Zhang, Neural network modeling and analysis of gel casting preparation of porous Si_3N_4 ceramics, Ceramics International 35 (2009) 2943–2950.
[11] S.Q. Ding, Y.P. Zeng, D.L. Jiang, Oxidation bonding of porous silicon nitride ceramics with high strength and low dielectric constant, Materials Letters 61 (2007) 2277–2280.
[12] K.H. Zuo, Y.P. Zeng, D.L. Jiang, The mechanical and dielectric properties of Si_3N_4-based sandwich ceramics, Materials and Design 35 (2012) 770–773.
[13] Y.S. Liu, L.F. Cheng, L.T. Zhang, Microstructure and properties of particle reinforced silicon carbide and silicon nitride ceramic matrix composites prepared by chemical vapor infiltration, Materials Science and Engineering A 475 (2008) 217–223.
[14] X.M. Li, X.W. Yin, L.T. Zhang, L.F. Cheng, Y.C. Qi, Mechanical and dielectric properties of porous Si_3N_4–SiO_2 composite ceramics, Materials Science and Engineering A 500 (2009) 63–69.

[15] X.M. Li, L.T. Zhang, X.W. Yin, Z.J. Yu, Mechanical and dielectric properties of porous Si_3N_4–SiC(BN) ceramic, Journal of Alloys and Compounds 490 (2010) L40–L43.

[16] H.S. Kim, M.K. Kim, S.B. Kang, S.H. Ahn, K.W. Nam, Bending strength and crack-healing behavior of Al_2O_3/SiC composites ceramics, Materials Science and Engineering A 483–484 (2008) 672–675.

[17] W. Nakao, M. Ono, S.K. Lee, K. Takahashi, K. Ando, Critical crack-healing condition for SiC whisker reinforced alumina under stress, Journal of the European Ceramic Society 25 (2005) 3649–3655.

[18] K. Houjyou, K. Ando, S.P. Liu, S. Sato, Crack-healing and oxidation behavior of silicon nitride ceramics, Journal of the European Ceramic Society 24 (2004) 2329–2338.

[19] S.R. Choi, V. Tikare, Crack healing behavior of hot pressed silicon nitride due to oxidation, Scripta Materialia 26 (1992) 1263–1268.

[20] X.H. Zhang, L. Xu, S.Y. Du, W.B. Han, J.C. Han, Crack-healing behavior of zirconium diboride composite reinforced with silicon carbide whiskers, Scripta Materialia 59 (2008) 1222–1225.

[21] X.H. Zhang, L. Xu, S.Y. Du, W.B. Han, J.C. Han, Preoxidation and crack-healing behavior of ZrB_2–SiC ceramic composite, Journal of the American Ceramic Society 91 (2008) 4068–4073.

[22] G.M. Song, Y.T. Pei, W.G. Sloof, S.B. Li, J.Th.M. De Hosson, S. van Der Zwaag, Oxidation-induced crack healing in Ti_3AlC_2 ceramics, Scripta Materialia 58 (2008) 13–16.

[23] G.M. Liu, M.S. Li, Y.C. Zhou, Y.M. Zhang, Influence of pre-oxidation on the hot corrosion of Ti_3SiC_2 in the mixture of Na_2SO_4–NaCl melts, Corrosion Science 48 (2006) 650–661.

[24] G.Q. Chen, R.B. Zhang, H. Zou, Thermal shock behavior of as-sintered and pre-oxidation $Zr_2Al_4C_5$–20SiC composites, Materials and Design 31 (4) (2010) 2167–2170.

[25] X.M. Li, X.W. Yin, L.T. Zhang, S.S. He, The devitrification kinetics of silica powder heat-treated in different conditions, Journal of Non-Crystalline Solids 354 (2008) 3254–3259.

[26] S.N. Karlsdottir, J.W. Halloran, C.E. Henderson, Convection patterns in liquid oxide films on ZrB_2–SiC composites oxidized at high temperature, Journal of the American Ceramic Society 90 (9) (2007) 2863–2867.

[27] J.D. Walton, Reaction sintered silica-nitride for high-temperature radome applications, American Ceramic Society Bulletin 53 (1974) 255–258.

[28] D. Kingery, H.K. Bowen, D.R. Uhlmann, Introduction to Ceramics, John & Wiley Sons Inc., New York, 1976.